

See discussions, stats, and author profiles for this publication at: <https://www.researchgate.net/publication/6117242>

# Ion Chemistry in Cold Plasmas of H<sub>2</sub> with CH<sub>4</sub> and N<sub>2</sub>

ARTICLE *in* THE JOURNAL OF PHYSICAL CHEMISTRY A · OCTOBER 2007

Impact Factor: 2.69 · DOI: 10.1021/jp073569w · Source: PubMed

---

CITATIONS

20

---

READS

43

6 AUTHORS, INCLUDING:



**I. Tanarro**

Spanish National Research Council

89 PUBLICATIONS 867 CITATIONS

SEE PROFILE



**Francisco L Tabares**

Centro Investigaciones Energéticas, Medioa...

273 PUBLICATIONS 1,731 CITATIONS

SEE PROFILE

# Ion Chemistry in Cold Plasmas of H<sub>2</sub> with CH<sub>4</sub> and N<sub>2</sub>

I. Tanarro,<sup>\*,†</sup> V. J. Herrero,<sup>\*,†</sup> A. M. Islyaikin,<sup>‡,§</sup> I. Méndez,<sup>†</sup> F. L. Tabarés,<sup>§</sup> and D. Tafalla<sup>§</sup>

*Instituto de Estructura de la Materia, CSIC, Serrano 123, 28006 Madrid, Spain and  
Association Euratom/Ciemat, Av. Complutense 22, 28040 Madrid, Spain*

*Received: May 10, 2007; In Final Form: July 10, 2007*

The distributions of ions and neutrals in low-pressure ( $\approx 10^{-2}$  mbar) DC discharges of pure hydrogen and hydrogen with small admixtures (5%) of CH<sub>4</sub> and N<sub>2</sub> have been determined by mass spectrometry. Besides the mentioned plasma precursors, appreciable amounts of NH<sub>3</sub> and C<sub>2</sub>H<sub>x</sub> hydrocarbons, probably mostly from wall reactions, are detected in the gas phase. Primary ions, formed by electron impact in the glow region, undergo a series of charge transfer and reactive collisions that determine the ultimate ion distribution in the various plasmas. A comparison of the ion mass spectra for the different mixtures, taking into account the mass spectra of neutrals, provides interesting information on the key reactions among ions. The prevalent ion is H<sub>3</sub><sup>+</sup> in all cases, and the ion chemistry is dominated by protonation reactions of this ion and some of its derivatives. Besides the purely hydrogenic ions, N<sub>2</sub>H<sup>+</sup>, NH<sub>4</sub><sup>+</sup>, and CH<sub>5</sub><sup>+</sup> are found in significant amounts. The only mixed C/N ion clearly identified is protonated acetonitrile C<sub>2</sub>H<sub>4</sub>N<sup>+</sup>. The results suggest that very little HCN is formed in the plasmas under study.

## 1. Introduction

Hydrogen is the dominant molecular species in interstellar space, and consequently, the ions H<sup>+</sup>, H<sub>2</sub><sup>+</sup>, and H<sub>3</sub><sup>+</sup> derived from this molecule play a key role in its gas-phase chemistry which, under the very low temperatures and densities typical of this medium, is essentially driven by ion–molecule reactions. In particular, the H<sub>3</sub><sup>+</sup> ion, relatively stable in interstellar space,<sup>1,2</sup> constitutes an excellent protonating agent<sup>3</sup> given the very low proton affinity of H<sub>2</sub> and high cross sections typical of ion–molecule encounters. It is generally assumed that H<sub>3</sub><sup>+</sup> forms the basis for an extensive network of ion–molecule processes involving initially light species containing mostly C, O, and N that are responsible for creation of many of the molecules observed in interstellar space (see refs 4–6 and references therein). In fact, only 13 ions have been positively identified in the interstellar medium,<sup>6</sup> but many others are postulated in current astrochemistry models.<sup>4,5</sup> Likewise, models of the ionospheres of the giant planets indicate that they are largely dominated by H<sup>+</sup> and H<sub>3</sub><sup>+</sup> in their upper layers. Other ions, mostly derived from reactions of H<sub>x</sub><sup>+</sup> with methane, begin to appear with decreasing altitude.<sup>7</sup>

Ion–molecule reactions of H<sub>x</sub><sup>+</sup> species and hydrocarbons are also important in other media of technological interest like those used in plasma-enhanced chemical vapor deposition (PECVD) of diamond-like and amorphous hydrogenated carbon (a-C:H) films.<sup>8–11</sup> In these cold plasmas, hydrogenic ions contribute to formation of C<sub>x</sub>H<sub>y</sub><sup>+</sup> species, which can play an important role in film formation. Although in many cases carbonaceous radicals are deemed the main film precursors, ion bombardment can help decisively to film growth through creation of dangling bonds and other reactive sites.<sup>12–14</sup> Depending on the circumstances,

ions can also contribute directly to film growth.<sup>15,16</sup> Both positive and negative carbonated ions are assumed to play a significant role in hydrocarbon nanoparticle nucleation.<sup>17</sup>

Molecular nitrogen or nitrogen-containing species were introduced in hydrocarbon plasmas in an attempt to synthesize crystalline  $\beta$ -C<sub>3</sub>N<sub>4</sub>, a material with predicted properties superior to those of diamond.<sup>18</sup> In spite of intense research efforts, no unambiguous experimental evidence of the production of this crystalline material was reported.<sup>19</sup> These investigations showed that incorporation of nitrogen to the growing carbon films is difficult; furthermore, the presence of nitrogen-containing species was found to hamper or preclude completely the deposition of hydrogenated carbon or carbon nitride compounds for a broad range of experimental conditions.<sup>20</sup> Inhibition of a-C:H film formation in the presence of nitrogenous species has been shown to be of interest for development of nuclear fusion reactors. Carbon-based materials exhibit the best general behavior against high thermal loads and other extreme conditions and are used in divertors and limiters in these devices.<sup>21</sup> Unfortunately, the high reactivity of carbon with hydrogenic isotopes, especially at high temperatures, leads to strong chemical sputtering which shortens the material lifetime and contributes to formation of a-C:H films, rich in deuterium and tritium proceeding from the fusion fuel. These deposits are formed in parts of the device not directly exposed to the hot plasma, especially in cold plasma regions after the divertor. In this way, radioactive tritium retention has become a major issue for the normal operation of next-step fusion reactors.<sup>21,22</sup> Encouraging results with moderate reductions of carbon redeposition induced by injection of nitrogen have already been obtained in actual fusion devices.<sup>20,23</sup> At present, the detailed mechanisms by which N-containing compounds hamper film growth are under debate. Various gas-phase and surface processes involving neutrals and ions are currently being considered.<sup>24–30</sup>

In spite of the evident relevance of all the plasmas mentioned in the previous paragraphs, the ionic composition and underlying

\* To whom correspondence should be addressed. E-mail: itanarro@iem.cfmac.csic.es, vherrero@iem.cfmac.csic.es.

<sup>†</sup> Instituto de Estructura de la Materia.

<sup>‡</sup> Present address: Mikron JSR, 1stZapadny Proezd 12/1, 124460 Zelenograd, Moscow, Russia.

<sup>§</sup> Association Euratom/Ciemat.

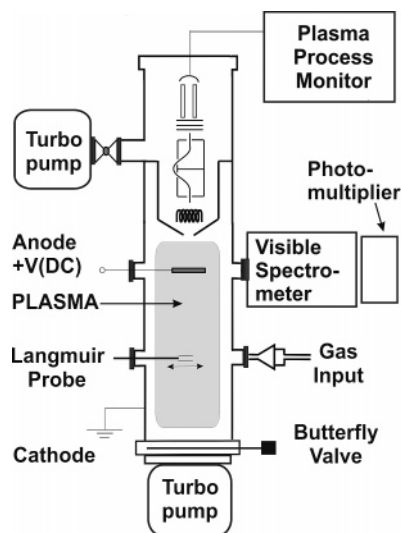


**Figure 1.** Schematic illustration of the experimental setup.

chemistry of hydrogen-dominated cold plasmas are often poorly known. Even pure hydrogen plasmas, apparently simple from a chemical point of view, may require consideration of a high number of processes due to the multiple interactions of neutral and charged particles and the various degrees of internal excitation of atoms and molecules (see refs 31–36 and references therein). A proper understanding of the ion chemistry of cold  $\text{H}_2$  plasmas will be best achieved through a combination of detailed experimental diagnostics and kinetic analysis. Two examples of this approach have been recently reported.<sup>37,38</sup> Hollmann and Pigarov<sup>37</sup> measured ion concentrations in a hydrogen reflex arc discharge characterized by high electron and ion densities ( $10^{11}$ – $10^{12}$   $\text{cm}^{-3}$ ). The results of these measurements were successfully modeled by the authors using a reduced set of rate equations and cross-section data from the literature. In a recent study<sup>38</sup> we investigated the plasmas produced in a low-pressure  $\text{H}_2$  DC hollow cathode (HC) discharge. Although they differ from the reflex-arc discharges, most notably in their electron density (which is of the order of  $10^{10}$   $\text{cm}^{-3}$  in the HC plasmas), a kinetic model using the same basic reactions considered by Hollmann and Pigarov<sup>37</sup> could account for the experimental observations. In our plasmas,  $\text{H}_2$  was found to have a high vibrational excitation, and  $\text{H}_3^+$  was the dominant ion when the ionic mean free path approached the dimensions of the glow. In the present work, we extend the previous investigation to more complex mixtures relevant for the plasmas mentioned in the previous paragraphs. In an attempt to identify key species and processes in the chemistry of hydrogenic ions with small hydrocarbons and nitrogen, we measured the mass spectra of the ions and neutrals present in HC discharges of pure  $\text{H}_2$  and mixtures of  $\text{H}_2$  with small amounts of either  $\text{CH}_4$  or  $\text{N}_2$  or with both compounds together. The results are analyzed and discussed in light of available kinetic data. Mass spectra of the neutral species in these plasmas were studied previously in a more detailed way by our group.<sup>27,29,39</sup>

## 2. Experimental Section

The experimental plasma reactor, shown in Figure 1, is basically the same as in our previous works on air and hydrogen plasmas.<sup>38,40,41</sup> It consists of a grounded cylindrical stainless steel vessel (10 cm diameter, 34 cm length) and a central anode. The vessel walls are provided with a number of ports for

connection of gas inlets, diagnostics tools, observation windows, and pressure gauges (not all shown in Figure 1).

The reactor was continuously pumped by a 450 L/s turbomolecular pump in series with a rotary pump to a base pressure of  $10^{-6}$  mbar. The desired reactor pressure and gas mixture composition were selected by balancing the input gas flow for each gas with a needle valve in the gas inlet. A total gas pressure of  $P = 0.02$  mbar  $\text{H}_2/\text{N}_2(0\text{--}5\%)/\text{CH}_4(0\text{--}5\%)$ , measured with a capacitance absolute manometer, was used. The stability of the composition in the various mixtures was additionally checked by measuring the peaks in the mass spectra of  $\text{H}_2$ ,  $\text{CH}_4$ , and  $\text{N}_2$  (see below). Residence times,  $\tau_{\text{res}}$ , of the various plasma precursors were determined by cutting suddenly with a quick connector the flow of each component to the reactor and monitoring its decay time by time-resolved mass spectrometry. Residence times of  $\sim 0.1$  s were measured for  $\text{CH}_4$  and  $\text{N}_2$ , and a value of  $\sim 0.4$  s was obtained for  $\text{H}_2$ . The differences are due to the distinct pumping speed of the turbomolecular pump for the diverse species. Plasma currents  $I_p \approx 150$  mA and supply voltages  $V \approx 400$  V were used in the discharges of pure  $\text{H}_2$  or  $\text{H}_2(5\%) \text{N}_2$ . In the mixtures containing (5%)  $\text{CH}_4$  the discharge current was seen to drop by about 20% and the voltage rose in the same proportion. In order to initiate the discharges at this low operation pressure, an electron gun built in our laboratory, consisting basically of a tungsten filament operating at 2 A and  $-2000$  V<sub>DC</sub>, was employed.

A Plasma Process Monitor, Balzers PPM421, was used for detection of both neutrals and ions from the plasma. It consists of an electron bombardment ionizer, an electrostatic focusing system, a cylindrical mirror energy analyzer, and a quadrupole mass filter with a secondary electron multiplier in the counting mode. The background signal from the PPM chamber was subtracted in the measurements of neutrals. For detection of ions, the electron bombardment ionizer is switched off and the ions are allowed to enter the detector directly from the plasma. The apparatus was installed in a differentially pumped chamber connected to the reactor through a  $100 \mu\text{m}$  diaphragm. During operation the pressure in the detection chamber was kept in the  $10^{-7}$  mbar range by means of a turbomolecular pump and a dry pump.

Ion fluxes were calculated by integrating the ion energy distributions recorded in the experiments for each individual mass value. These energy distributions were essentially concentrated in a large and sharp maximum (fwhm  $\approx 2$  V) at energies very close to that of the discharge potential. Some of them also had a broad and weak tail extending to lower potentials. The relative sensitivity of the plasma monitor (including electrical filters and electron multiplier) to the different ion masses was checked by filling the chamber of the PPM421 with a small pressure of  $\text{H}_2$ , He, Ne, Ar, and Xe and comparing in each case the PPM signal, weighted by the respective ionization cross section at the chosen electron energy (70 eV), with the chamber pressure as determined from the reading of a Bayard–Alpert gauge with the appropriate correction factor. As shown by Pecher,<sup>42</sup> this calibration procedure is also adequate for ions extracted from the plasma. The calibration led to a sensitivity dependence roughly proportional to  $m^{-0.5}$ , in agreement with other authors.<sup>42,43</sup>

The radial distribution of electron mean temperature and total charge density in the cylindrical reactor were measured with a double Langmuir probe built in our laboratory<sup>44</sup> by assuming a collision-free probe sheath and orbital limited motion.<sup>45</sup> It is also tacitly assumed that negative ions are negligible in the

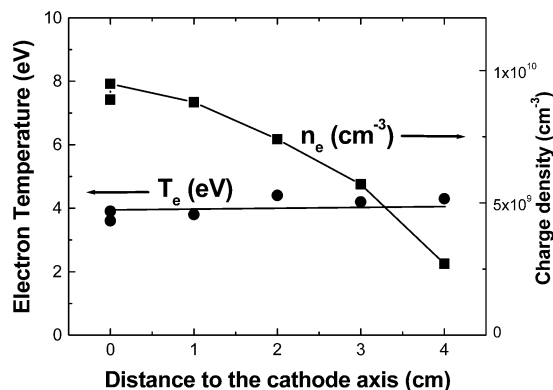


**Figure 2.** Radial distribution of electron energy (dots) and charge density (squares) in a 150 mA, 0.02 mbar, 1% N<sub>2</sub>/1% CH<sub>4</sub>/H<sub>2</sub> discharge, measured with a double Langmuir probe. Lines are only to guide the eye.

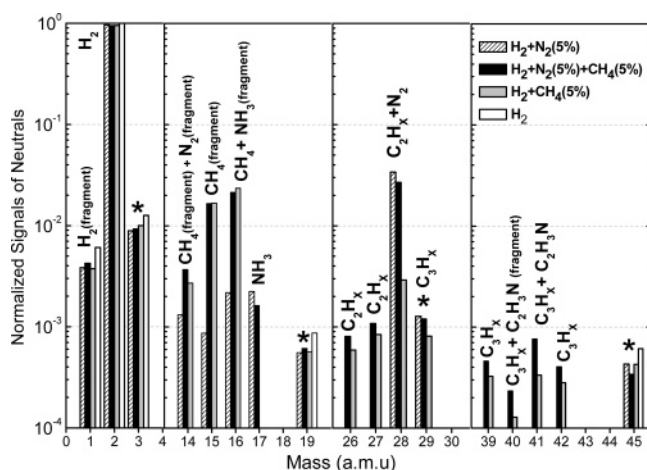


**Figure 3.** Normalized intensities of neutrals detected with the PPM in the plasma for the four different precursor mixtures. The peaks corresponding to the fragmentation pattern by electron bombardment in the PPM of the main compounds are identified in the figure. Peaks marked with an asterisk do not correspond to molecules from the plasma but mainly to species formed by reactions involving hydrogen ions in the ionizer of the PPM (see text).

plasmas studied and that electroneutrality is brought about by a balance between the density of electrons and that of positive ions.

### 3. Results

Figure 2 shows the double Langmuir probe results obtained for a 150 mA, 0.02 mbar, H<sub>2</sub>/N<sub>2</sub>(5%)/CH<sub>4</sub>(5%) discharge as a function of the distance to the cathode axis. The electron mean temperature, 4 eV, did not change with radial position. The charge density had a maximum of  $\sim 10^{10}$  cm<sup>-3</sup>, coinciding with the axis of symmetry of the cylindrical cathode, and decreased toward the cathode wall, as expected for DC glow discharges.<sup>46</sup> With gas densities  $\sim 5 \times 10^{14}$  cm<sup>-3</sup>, the maximum ionization degree was then  $\sim 10^{-4}$ . An equivalent series of Langmuir probe measurements at a different axial position was obtained too with the probe put through a flange available at the level of the anode and led to similar results. For the rest of the discharges analyzed, the results were similar and laid in all cases within the experimental uncertainty ( $\sim 30\%$ ).

Figure 3 shows the normalized mass spectra of the neutral species present in each of the four discharges investigated,

detected as ions formed by electron bombardment of the neutrals in the ionizer of the PPM. These signals are thus proportional to the number density of the various gas molecules but affected by fragmentation. Peaks marked with an asterisk in Figure 3 at  $m/q = 3, 19, 29$ , and  $45$  are essentially due to protonated ions formed in the ionizer of the mass spectrometer in reactions of hydrogenic ions with H<sub>2</sub> and with the background molecules: water, CO, and CO<sub>2</sub>. These peaks are also observed when the discharge is off, and disappear from the PPM when H<sub>2</sub> is removed. The peak at mass 29 may be also due in part to fragmentation of C<sub>3</sub>H<sub>x</sub>.

All discharges are dominated by the peak  $m/q = 2$ , corresponding to hydrogen molecules, which is always the dominant species. In the H<sub>2</sub>/CH<sub>4</sub> plasma, three more groups of peaks are found at  $m/q = 14\text{--}17$ ,  $26\text{--}29$ , and  $39\text{--}42$ ; the intensity of the maximum signals in each group of peaks decreases roughly by an order of magnitude with increasing  $m/q$ . The first group is dominated by peaks at  $m/q = 15$  and  $16$  formed in the direct and dissociative ionization of CH<sub>4</sub>. The other two groups of peaks correspond to C<sub>2</sub>H<sub>x</sub> and C<sub>3</sub>H<sub>x</sub> molecules formed in the plasma reactor, but the assignment of the individual peaks is not straightforward due to the complex fragmentation patterns of the various C<sub>2</sub>H<sub>x</sub> and C<sub>3</sub>H<sub>x</sub> hydrocarbons and requires a careful analysis<sup>29,48</sup> which is not attempted here. For the type of plasmas used in the present experiments, the main C<sub>2</sub>H<sub>x</sub> species have been shown to be acetylene and ethylene.<sup>29,39</sup> The lowest intensity peaks, between 39 and 42, correspond to C<sub>3</sub>H<sub>x</sub> molecules. In the H<sub>2</sub>/N<sub>2</sub> plasma, the N<sub>2</sub> molecules give rise to a distinct peak at  $m/q = 28$  and a smaller one at mass 14 corresponding to N<sup>+</sup>; two peaks at  $m/q = 17$  and  $16$  are attributed to the direct and dissociative ionization of NH<sub>3</sub> generated in the discharge chamber. The spectrum of the H<sub>2</sub>/N<sub>2</sub>/CH<sub>4</sub> plasma is essentially the sum of the contributions of those corresponding to H<sub>2</sub>/N<sub>2</sub> and H<sub>2</sub>/CH<sub>4</sub>. No clear indication of formation of mixed C/N species can be deduced from the mass spectra of neutrals. The primary candidate of this kind of mixed species would be HCN ( $m/q = 27$ ), but this peak also corresponds to daughter ions of hydrocarbons, and previous analyses have shown that, for the plasmas under study, formation of C<sub>2</sub>H<sub>x</sub> is enhanced by addition of N<sub>2</sub> and that HCN is produced in very small amounts.<sup>29,39</sup> A hint of formation of acetonitrile is found in the signals at masses 40 and 41, corresponding to the main fragment and the parent ion of C<sub>2</sub>H<sub>3</sub>N, which seem to be comparatively larger in the H<sub>2</sub>/CH<sub>4</sub>/N<sub>2</sub> discharge than in the H<sub>2</sub>/CH<sub>4</sub> one. Although the peaks in this mass range are too weak to make a firm assertion, analysis of the ion spectra (see below) supports this conclusion.

The normalized flux distributions of the plasma ions reaching the cathode have been represented in Figure 4 up to  $m/q = 30$  for the four discharges investigated. The typical uncertainty in the total amplitudes of the measured flux signals after averaging four sets of data for each gas mixture is  $\sim 30\%$ , although the uncertainty in the relative intensities among the different peaks is much lower ( $\sim 10\%$ ). Minor peaks corresponding to higher  $m/q$  values were also found and will be discussed below. The observed ion flux distributions contain not only the fragment ions of the precursor gases produced in the process of electron impact in the gas discharge, but also a variety of other peaks indicative of chemical reactions within the plasma. Although the present measurements do not strictly allow a distinction between ions of different composition having the same  $m/q$  value, joint consideration of the different plasma mixtures can shed some light on this point. Throughout the discussion we will assume that ions are single charged.



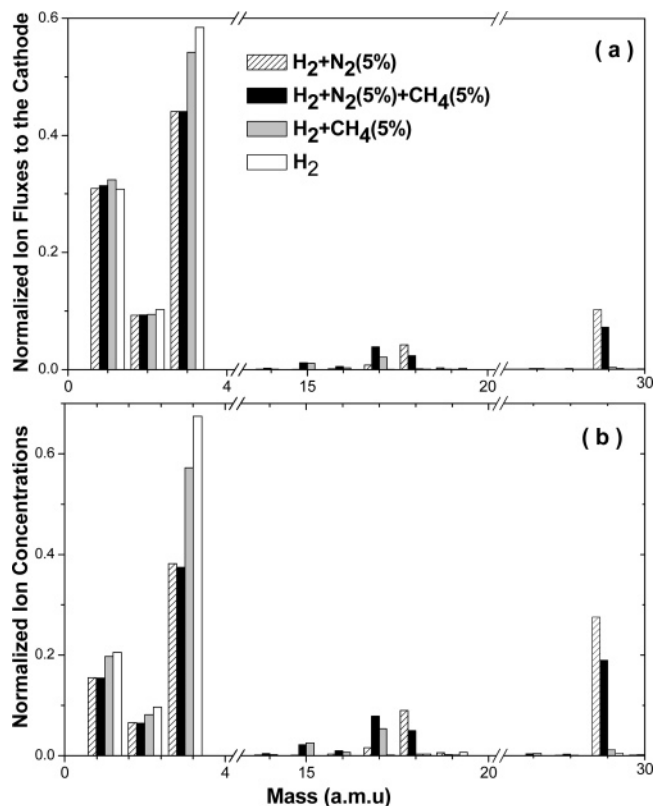


**Figure 4.** (a) Flux distributions of the ions reaching the cathode normalized to one for the four discharges investigated: pure  $\text{H}_2$ , and  $\text{H}_2$  mixed with 5%  $\text{N}_2$ , 5%  $\text{CH}_4$ , and 5%  $\text{N}_2$  + 5%  $\text{CH}_4$ . (b) Normalized to one concentrations of ions in the plasma corresponding to the discharges of the upper panel (4a) (see text). For identification of the different ions, see text and Figure 5.

Hydrogenic ions, in particular ions with  $m/q = 3$  ( $\text{H}_3^+$ ), were found to be preponderant in all cases, in accordance with the expectations for the conditions of this type of plasmas whose composition is essentially dominated by molecular hydrogen.<sup>37,38,48</sup> In plasmas containing  $\text{CH}_4$  or  $\text{N}_2$  appreciable contributions from masses higher than three can be observed. Note, in particular, the change in the ion flux distribution in nitrogen-containing plasmas, where a peak at  $m/q = 29$  accounts for 8–10% of the ion flux and where the contribution of  $\text{H}_3^+$  ions is reduced by about 20% with respect to that of pure hydrogen plasmas. Ion peaks between 1% and 5% are observed at masses 15, 17, and 18.

Instead of ion fluxes, Figure 4b shows the estimated distributions of ion concentrations (volume densities) in the plasma for the various discharges considered. The flow of ions from the plasma to the cathode is regulated by their Bohm velocity,<sup>46</sup> which is inversely proportional to the square root of the ion mass. Consequently, in order to derive the ion concentrations in the plasma, the ion flux signals corresponding to a given mass,  $m_i$ , were multiplied by  $m_i^{0.5}$ . Note that due to their comparatively small flow velocity, heavier ions tend to concentrate in the plasma. In particular, in the  $\text{N}_2$ -containing plasmas the ions of mass 29 contribute largely to the total ion concentration. We will focus the following discussion on concentrations rather than on cathode fluxes, since they are more meaningful for the ion chemistry within the plasma.

A large number of ions contributing less than 1% to the total ion concentration can be also observed in a logarithmic scale in Figure 5, where all significant signals in the  $m/q = 0$ –45 range have been represented. Some weaker peaks were also found at higher masses, but their contribution to the global ion

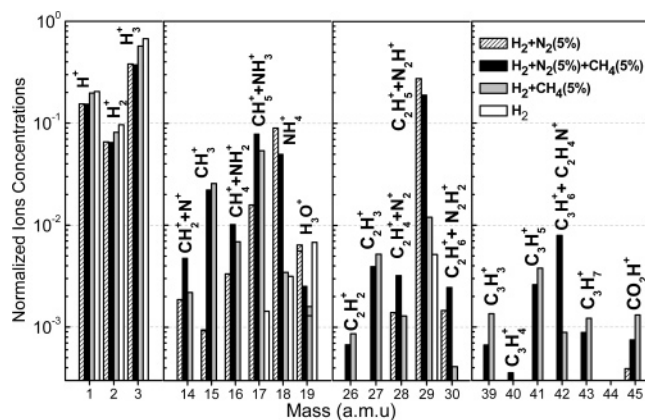


**Figure 5.** Normalized ion concentrations in semilogarithmic scale extended up to 46 amu in the same conditions of Figure 4. The ions corresponding to the various  $m/q$  values are identified in the figure. When more than one ion can contribute to a given  $m/q$  value, the preponderant species is written first (see text).

density is negligible and will not be considered. Leaving aside pure hydrogenic ions,  $m/q = 18$  ( $\text{NH}_4^+$ ) and 29 ( $\text{N}_2\text{H}^+$ ) were found to be prevalent in the  $\text{H}_2$  + (5%) $\text{N}_2$  plasmas; whereas in the  $\text{H}_2$  + (5%) $\text{CH}_4$  discharges  $m/q = 15$  ( $\text{CH}_3^+$ ) and  $m/e = 17$  ( $\text{CH}_5^+$ ) were seen to dominate. The same ions are found to be dominant in other types of methane discharges,<sup>49,50</sup> and a similar decrease in  $\text{H}_3^+$ , accompanied by a growth in  $\text{CH}_5^+$  upon addition of a small amount of  $\text{CH}_4$  to a capacitively coupled  $\text{H}_2$  discharge, has been recently reported.<sup>50</sup> Smaller ion peaks with intensities below 0.5% appeared mostly grouped in clusters of  $m/q = 14$ –19, 26–30, and 39–45. The first two of these clusters correspond to  $\text{C}_x\text{H}_y^+$  ions with  $x = 1$  and 2. The third cluster is due mostly to  $\text{C}_3\text{H}_y^+$  ions. The peaks of hydrocarbon ions,  $\text{C}_x\text{H}_y^+$ , decrease in intensity with growing carbon number, as expected for typical low-pressure cold plasmas containing methane.<sup>42,51</sup> With increasing methane pressure, the number of ions with more carbon atoms grows significantly.<sup>8,42</sup> Identification of ion peaks in  $\text{H}_2$  +  $\text{N}_2$  +  $\text{CH}_4$  gas mixtures is more difficult than in the two binary mixtures, since some of the ion peaks could have contributions from  $\text{N}_x\text{H}_y^+$ ,  $\text{C}_x\text{H}_y^+$ , and even  $\text{C}_x\text{N}_y\text{H}_z^+$  species.<sup>51,52</sup> By comparing the peak measured for a given  $m/q$  value in the various gas mixtures, some of the signals could be assigned unambiguously to carbon or nitrogen ions. This was the case of  $m/q = 15$  ( $\text{CH}_3^+$ ), 26 ( $\text{C}_2\text{H}_2^+$ ), and 27 ( $\text{C}_2\text{H}_3^+$ ), which were absent, or more than 1 order of magnitude weaker, when  $\text{CH}_4$  was not added to the precursor gas. Among them,  $\text{CH}_3^+$  was always the major one. The same behavior was observed for heavier ions like 39 ( $\text{C}_3\text{H}_3^+$ ), 41 ( $\text{C}_3\text{H}_5^+$ ), and 43–( $\text{C}_3\text{H}_7^+$ ). For the same reason, the prominent peaks at  $m/q = 18$  and 29 must be due to the nitrogenic ions  $\text{NH}_4^+$  and  $\text{N}_2\text{H}^+$ . Some other masses in the ion spectra of the ternary mixture could not be assigned to a single ion but to the additive contribution of  $\text{N}_x\text{H}_y^+$  and  $\text{C}_x\text{H}_y^+$  species, since they have significant intensities in the three mixtures. This was the situation for  $m = 14$  ( $\text{N}^+ + \text{CH}_2^+$ ), 16 ( $\text{CH}_4^+ + \text{NH}_2^+$ ), 17 ( $\text{CH}_5^+ + \text{NH}_3^+$ ), 28 ( $\text{N}_2^+ + \text{C}_2\text{H}_4^+$ ), 29 ( $\text{N}_2\text{H}^+ + \text{C}_2\text{H}_5^+$ ), and 30 ( $\text{N}_2\text{H}_2^+ + \text{C}_2\text{H}_6^+$ ). Among them, the largest contribution to carbon ions was undoubtedly that of mass 17 (mainly  $\text{CH}_5^+$ ), which exceeded the concentration of  $\text{CH}_3^+$  in all cases. Comparison of the signal intensities corresponding to  $m/q = 28$ , 29, and 39 in the different mixtures suggests a negligible contribution of  $\text{C}_x\text{NH}_z^+$  mixed C–N ions. Nevertheless, a single hybrid C–N ion was clearly identified at  $m = 42$  ( $\text{C}_2\text{H}_4\text{N}^+$ ); this peak was only significant in the  $\text{H}_2/\text{N}_2(5\%)/\text{CH}_4(5\%)$

mixture and decreased by at least 1 order of magnitude when either N<sub>2</sub> or CH<sub>4</sub> were removed from the feed gas.

#### 4. Discussion

**Gas-Phase Neutrals and Wall Processes.** Before starting the discussion on ion chemistry, which is the main objective of the present work, we will make some general comments on the neutral species observed in our discharges and on their likely origin.

Under our experimental conditions, with a discharge power of  $\sim 50$  W, a discharge volume of  $\sim 3$  l, and residence times of the molecules in the reactor  $\tau_{\text{res}} \approx 0.1$  s for N<sub>2</sub> and CH<sub>4</sub> and  $\tau_{\text{res}} \approx 0.4$  s for H<sub>2</sub>, a low dissociation degree ( $\sim 5\%$  for N<sub>2</sub> and  $\sim 15\%$  for CH<sub>4</sub> and H<sub>2</sub>) was obtained in the plasmas under study; as a consequence, the gas composition is dominated by the plasma precursors (H<sub>2</sub>, CH<sub>4</sub>, and N<sub>2</sub>) and only small amounts of other compounds (NH<sub>3</sub>, C<sub>x</sub>H<sub>y</sub>) are found in the mass spectra, as shown in Figure 3. The concentrations of NH<sub>3</sub> and C<sub>2</sub>H<sub>x</sub> molecules are about 1 order of magnitude lower than those of N<sub>2</sub> and CH<sub>4</sub>.

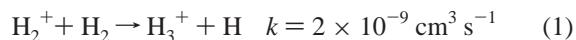
Different mechanisms including gas-phase and surface reactions could be, in principle, responsible for formation of the minor neutral species, but the present data do not allow a determination of the actual production mechanisms. Gas-phase generation of C<sub>x</sub>H<sub>y</sub> hydrocarbons and NH<sub>3</sub> molecules would require bimolecular reactions between molecules and radicals with typical rate constants in the  $10^{-10}$ – $10^{-11}$  cm<sup>3</sup> s<sup>-1</sup> range.<sup>17,53</sup> The contribution of this channel depends on the concentrations of radicals, which could not be determined in the present experiments. Gordiets et al.<sup>53–55</sup> constructed a detailed kinetic model for low-pressure H<sub>2</sub>/N<sub>2</sub> plasmas, including both gas-phase and surface processes, and concluded that surface reactions of physisorbed H and N atoms and NH<sub>x</sub> species are needed to account for the observed NH<sub>3</sub> formation in a variety of experiments. Although their results cannot be directly extrapolated to the present case, they stress the likelihood of heterogeneous processes for formation of ammonia in similar plasmas. Efficient NH<sub>3</sub> formation at metallic walls has also been reported in experiments with expanding arch-jet plasmas.<sup>56</sup> Gas-phase formation of NH<sub>3</sub> is not favored at the low pressures of our experiments, since it requires successive or three body collisions.<sup>53</sup> In plasmas with methane, C-containing radicals can also lead through successive collisions to formation of C<sub>x</sub>H<sub>y</sub> species,<sup>17,57</sup> but again this mechanism is not favored at low pressure, especially for the heavier C<sub>x</sub>H<sub>y</sub> molecules. In these plasmas carbonaceous films are deposited at the walls. Interactions of these films with reactive plasma species can also lead to the release of C<sub>x</sub>H<sub>y</sub> neutral molecules.<sup>8,42</sup> The situation is even more complex for plasmas with CH<sub>4</sub> and N<sub>2</sub>, where nitrogen-containing compounds can interfere in different ways with formation and growth of the carbonaceous films, eventually giving rise to production of volatile compounds containing C or N atoms or both. The detailed comprehension of all these issues, which are nowadays the subject of intense research (see refs 22–29, 30, and 39 and references therein) is beyond the scope of this study, which is rather centered on the ion chemistry of small amounts of carbonaceous and nitrous molecules in low-pressure plasmas dominated by hydrogen.

**Ion Chemistry.** Primary ions in the plasmas are produced by electron impact ionization of the neutral precursors. These ions can then undergo charge transfer or reaction processes through collisions with neutral molecules before reaching the plasma sheath, where they are accelerated toward the cathode. Ion–molecule reactions of the species of interest have very large

rate constants<sup>58–60</sup> and are relevant, even under the low collision conditions typical of the present experiments ( $P \approx 0.02$  mbar,  $T_g \approx 300$  K, reactor radius = 5 cm). In addition, the cathode wall acts as an effective cation sink, preventing release of positively charged species from its surface, which implies that the measured distributions of ion concentrations are entirely a consequence of electronic and ionic collisions within the plasma. Moreover, these distributions are largely due to ion–molecule reactions, whose rate constants, mostly in the  $10^{-9}$  cm<sup>3</sup> s<sup>-1</sup> range,<sup>58,59</sup> compete favorably with those of electron impact ionization, which for the electronic temperatures of our discharges ( $\sim 4$  eV) are in the  $\sim 10^{-10}$  cm<sup>3</sup> s<sup>-1</sup> range.<sup>38,41,60–62</sup> It is useful to recall at this point the hierarchy of concentrations of the various chemical species in the plasmas. Hydrogen molecules have a density of  $\sim 5 \times 10^{14}$  cm<sup>-3</sup>, and the concentrations of N<sub>2</sub> and CH<sub>4</sub> are 20 times lower ( $\sim 2.5 \times 10^{13}$  cm<sup>-3</sup>). C<sub>2</sub>H<sub>x</sub> and NH<sub>3</sub> have densities of  $\sim 1$ – $2 \times 10^{12}$  cm<sup>-3</sup>. The concentrations of charged particles are much lower; the total electron density is  $\sim 10^{10}$  cm<sup>-3</sup>, and those of the individual positive ions range from  $\sim 7 \times 10^9$  to  $10^7$  cm<sup>-3</sup>. Characteristic times,  $\tau$ , for the reaction of ions with neutrals ( $\tau = 1/k \cdot [X]$ , where  $k$  is the reaction coefficient and  $[X]$  the neutral's concentration) will thus be in the tens of microseconds, of the same order than the time needed by ions to reach the cathode<sup>38,41</sup> and much shorter than the residence time of neutrals in the reactor (0.1–0.4 s). Electron impact neutralization plays a minor role in the depletion of plasma ions in our glow discharges. With typical rate coefficients in the  $10^{-8}$  cm<sup>3</sup> s<sup>-1</sup> range at the relevant electronic temperatures,<sup>37,63,64</sup> the characteristic times for electron impact neutralization are in the millisecond range, and thus much slower than most ion–molecule reactions. As indicated above, the chemistry of neutrals, with gas-phase bimolecular rate coefficients much smaller than those of ion–molecule reactions,<sup>17,65,66</sup> is probably dominated by surface processes.

In the following we will describe in some detail the likely chemistry of the different groups of ions observed in our experiments. The ion temperatures could not be measured in the present work, but given the experimental conditions, they should not be much higher than that of the neutrals ( $\sim 300$  K). Throughout the discussion the given rate coefficients refer to the room-temperature values from the critical compilations of Anicich.<sup>58,59</sup> Even if the ion temperatures were somewhat higher, the rate constant values would not be much affected, since rate constants for barrierless reactions of this type show only a weak dependence on temperature.

**Ions of Masses 1–3.** The processes of formation and interconversion of the three hydrogenic ions in a low-pressure DC plasma of pure H<sub>2</sub> were addressed in detail in ref 38, and only the details pertinent to the present measurements will be commented on here. In all the plasmas considered the dominant ion is H<sub>3</sub><sup>+</sup> formed in the reaction.

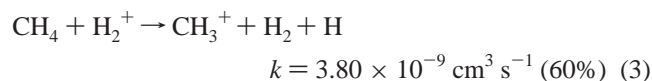
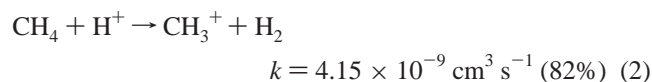


Most of the H<sub>2</sub><sup>+</sup> ions directly formed by electron impact ionization of the H<sub>2</sub> precursor are transformed to H<sub>3</sub><sup>+</sup> through reaction 1. H<sup>+</sup> ions are formed in the electron impact dissociative ionization of H<sub>2</sub> and in the electron impact ionization of H atoms that can reach relatively high concentrations within these plasmas.<sup>38</sup> Note that neither H<sub>3</sub><sup>+</sup> nor H<sup>+</sup> are lost through reactions with molecular hydrogen, which is the dominant plasma species. However, the three hydrogenic ions can react with other compounds present in the discharge, as we

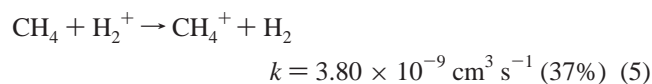
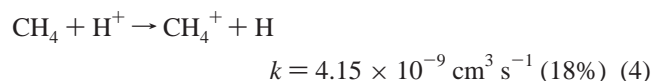
will see below. A pronounced drop in the  $\text{H}_3^+$  concentration upon addition of  $\text{CH}_4$  to pure  $\text{H}_2$  plasmas has been recently reported by Lombardi et al.<sup>10</sup> in a model of a MW discharge for diamond deposition. Figure 4 shows the marked decrease in the relative concentrations of  $\text{H}^+$ ,  $\text{H}_2^+$ , and  $\text{H}_3^+$  in our discharges, observed upon addition of a small amount of  $\text{CH}_4$ ,  $\text{N}_2$ , or both. The drop is most pronounced in the case of  $\text{H}_3^+$ , especially in plasmas containing  $\text{N}_2$ . In diffuse interstellar clouds its main destruction channel seems to be neutralization by electrons.<sup>2</sup> However, as indicated above, this mechanism is not relevant in our plasmas (see discussion in ref 38) and  $\text{H}_3^+$  is lost in reactions with neutrals and in wall collisions at the cathode, where it constitutes the main component of the global ion flux.

**Ions of Masses 14–19.** The peaks of masses 15, 16, and 17 are much larger in methane-containing plasmas. They correspond to  $\text{CH}_3^+$ ,  $\text{CH}_4^+$ , and  $\text{CH}_5^+$  ions that are readily formed in collisions of  $\text{H}^+$ ,  $\text{H}_2^+$ , and  $\text{H}_3^+$  with methane. In addition,  $\text{CH}_3^+$  and  $\text{CH}_4^+$  can be directly produced in the electron impact ionization of  $\text{CH}_4^+$ . The rate constants and branching ratios (in parentheses) for the most relevant ion–molecule reactions are listed here.

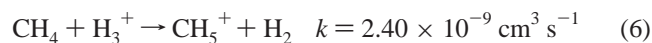
### $\text{CH}_3^+$



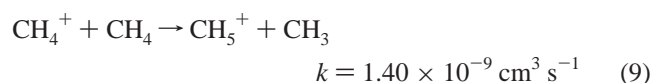
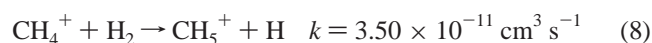
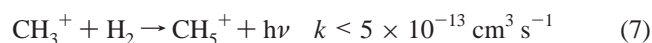
### $\text{CH}_4^+$



### $\text{CH}_5^+$

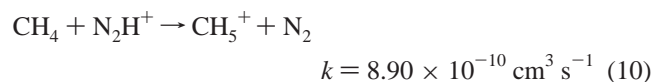


In addition,  $\text{CH}_5^+$  can be formed in collisions of  $\text{CH}_3^+$  and  $\text{CH}_4^+$  with hydrogen and methane



The remarkable structural and reactive properties of the  $\text{CH}_5^+$  ion have deserved attention by many research groups (see refs 67–69 and references therein). Although it has not yet been detected in interstellar space,<sup>6</sup> its presence has been often hypothesized in astrochemistry models. In particular, the radiative association process (eq 7) is thought to play an important role in starless core regions,<sup>4</sup> where the protonated methane formed can undergo dissociative recombination to produce various hydrocarbon species. However, the rate constant is too small and, in spite of involving collisions with  $\text{H}_2$ , which is the most abundant species in the discharges of the present study,

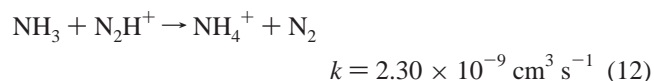
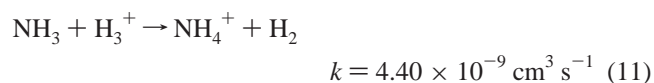
reaction 7 does not contribute appreciably to the destruction of  $\text{CH}_3^+$  or formation of  $\text{CH}_5^+$ . In contrast, reactions 8 and 9 contribute somewhat to the total production of  $\text{CH}_5^+$  and destroy a significant amount of the  $\text{CH}_4^+$  ions formed in reactions 4 and 5. The branching ratios of reactions 2 and 4 and 3 and 5 indicate that formation of  $\text{CH}_3^+$  is favored as compared with  $\text{CH}_4^+$ . This fact and the more efficient destruction pathways for  $\text{CH}_4^+$  justify the relative concentrations of  $\text{CH}_3^+$  and  $\text{CH}_4^+$  observed in the measurements.  $\text{CH}_5^+$ , the prevailing carbonated ion in the plasmas studied, is basically generated through reaction 6 in collisions of methane with the most abundant ion,  $\text{H}_3^+$ . In mixed plasmas with  $\text{CH}_4$  and  $\text{N}_2$  there is an additional production channel



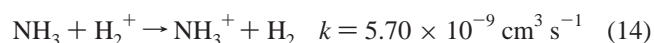
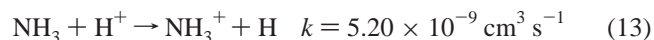
implying collisions of methane with the dyazenilium ion,  $\text{N}_2\text{H}^+$ , which is the second ion in importance in the nitrogenated discharges considered in this work, as shown in Figure 5 and discussed in the next paragraph. Note that due to reaction 10 the relative concentration of  $\text{N}_2\text{H}^+$  decreases and that of  $\text{CH}_5^+$  increases in the plasmas with  $\text{H}_2$ ,  $\text{CH}_4$ , and  $\text{N}_2$  as compared with the respective concentrations in the plasmas containing just  $\text{H}_2$  and  $\text{N}_2$  or  $\text{H}_2$  and  $\text{CH}_4$ . All the  $\text{CH}_x^+$  ions discussed thus far can react with  $\text{NH}_3$  or  $\text{C}_2\text{H}_x$ , molecules which appear as secondary products in the discharges under consideration (see below).

In Figure 5 the largest ion peak in the 15–19 interval is found at  $m/e = 18$  for the  $\text{H}_2/\text{N}_2$  discharge. This peak is due to the ammonium ion  $\text{NH}_4^+$ , which is formed mainly through the following reactions

### $\text{NH}_4^+$



Other minor channels leading to formation of  $\text{NH}_4^+$  involve reactions of  $\text{NH}_3^+$  with  $\text{H}_2$  and  $\text{CH}_4$  and of  $\text{CH}_x^+$  with  $\text{NH}_3$ .<sup>58,59</sup> Formation of significant amounts of  $\text{NH}_3$  as a result of heterogeneous wall reactions in low-pressure  $\text{H}_2/\text{N}_2$  plasmas is well documented in the literature (see refs 53–56 and references therein). Under the conditions of our discharges, the concentration of  $\text{NH}_3$  amounts roughly to 10% of the concentration of  $\text{N}_2$  or methane. The relatively high  $\text{NH}_4^+$  density observed, which is of the same order than that of the most intense carbonated ion,  $\text{CH}_5^+$ , is thus surprising at first sight; however, the ammonium ion is very stable and, unlike  $\text{CH}_x^+$  ions, does not react appreciably with  $\text{H}_2$ ,  $\text{N}_2$ , or the hydrocarbons present in the discharges.<sup>58,59</sup> The signal at mass 17 in  $\text{N}_2/\text{H}_2$  plasmas is due to  $\text{NH}_3^+$  and formed partly through direct electron ionization and partly in the reactions



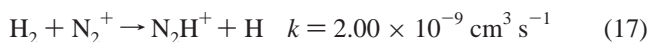
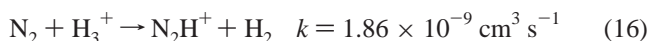
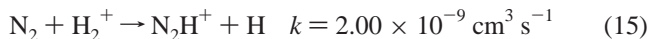
Minor contributions of ions from electron impact ionization of  $\text{CH}_4$ ,  $\text{N}_2$ , and  $\text{NH}_3$  are found at masses 14 ( $\text{CH}_2^+$ ,  $\text{N}^+$ ), 15 ( $\text{NH}^+$ ), and 16 ( $\text{NH}_2^+$ ). At  $m/q = 19$ , residual water molecules



in the chamber give a weak signal corresponding to protonated water, H<sub>3</sub>O<sup>+</sup>, in the four plasmas investigated.

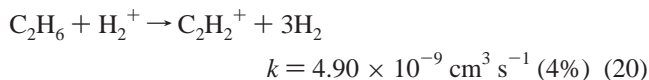
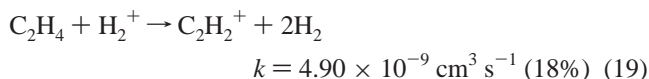
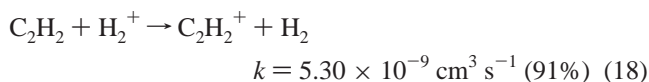
**Ions of Masses 26–30.** In the N<sub>2</sub>-containing discharges a very intense peak appears at  $m/q = 29$ . This peak, which is the second in intensity of the whole spectrum, corresponds to the dyazenilium ion formed in the reactions.

### N<sub>2</sub>H<sup>+</sup>

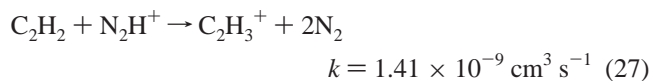
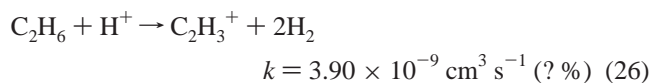
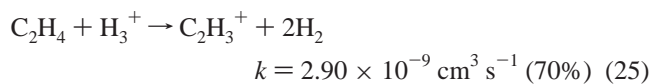
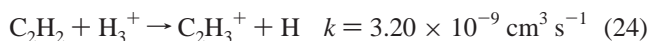
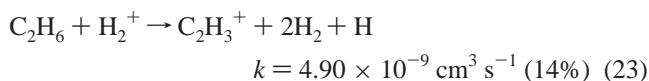
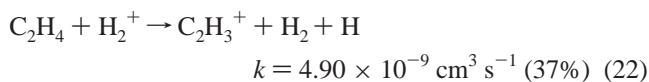
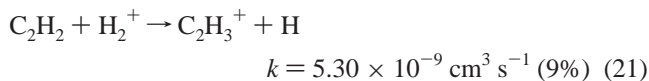


The three formation channels are efficient, in particular reactions 16 and 17 which involve the most abundant plasma ion (H<sub>3</sub><sup>+</sup>) and neutral species (H<sub>2</sub>), respectively. Due to its comparatively high mass, the flow of N<sub>2</sub>H<sup>+</sup> to the cathode is slow and its concentration is enriched in the plasma. The dyazenilium ion has been directly observed in interstellar clouds where it is often used in conjunction with collisional radiative models to derive the abundance of molecular nitrogen, which cannot be directly detected with the usual astrophysical spectroscopic techniques (see refs 6 and 70 and references therein). Once formed N<sub>2</sub>H<sup>+</sup> does not react with H<sub>2</sub> or N<sub>2</sub> but reacts with CH<sub>4</sub> (reaction 10) and other hydrocarbons, as shown below. Ions of C<sub>2</sub>H<sub>x</sub><sup>+</sup> are mainly formed by electron impact or in ion–molecule reactions of C<sub>2</sub>H<sub>x</sub> neutrals (especially C<sub>2</sub>H<sub>2</sub> and C<sub>2</sub>H<sub>4</sub> in the present case). Consequently, their concentration is in general lower than that of CH<sub>x</sub><sup>+</sup> species. Hydrogenic ions and N<sub>2</sub>H<sup>+</sup> are again the protonating agents. The main C<sub>2</sub>H<sub>x</sub><sup>+</sup> formation reactions and their respective branching ratios, in parentheses, are listed here.

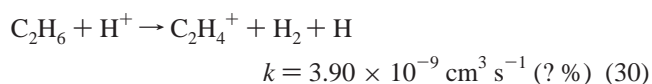
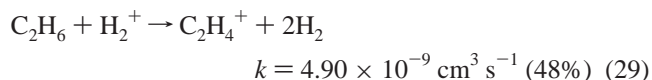
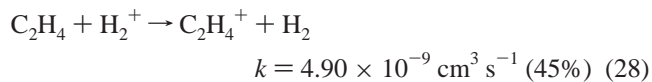
### C<sub>2</sub>H<sub>2</sub><sup>+</sup>



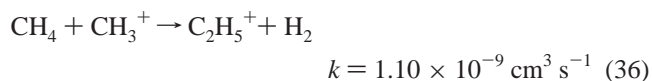
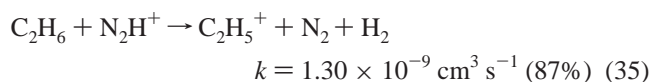
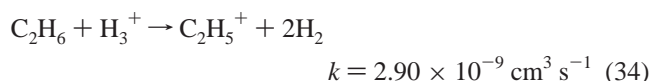
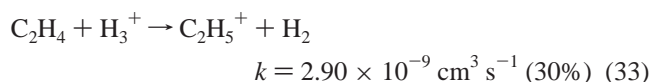
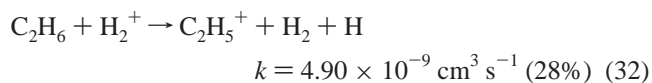
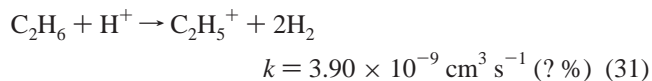
### C<sub>2</sub>H<sub>3</sub><sup>+</sup>



### C<sub>2</sub>H<sub>4</sub><sup>+</sup>



### C<sub>2</sub>H<sub>5</sub><sup>+</sup>

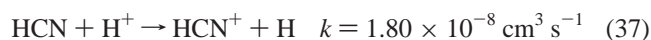


Reaction 36 is particularly interesting, since it describes a process of molecular aggregation giving rise to a higher mass hydrocarbon ion. Collisions of this type have been found to be determinant for the ion distributions in plasmas with higher methane pressures<sup>8,42</sup> which can be dominated by C<sub>y</sub>H<sub>x</sub><sup>+</sup> ions with  $y$  values higher than 1. In the present case, reaction 36 may contribute appreciably to C<sub>2</sub>H<sub>5</sub><sup>+</sup> formation. The branching ratios for the different channels of the C<sub>2</sub>H<sub>6</sub> reaction with H<sup>+</sup>, corresponding to processes 26, 30, and 31, are not given in the compilations of Anicich<sup>58,59</sup> and have been signaled with a question mark. Note that C<sub>2</sub>H<sub>2</sub><sup>+</sup> and C<sub>2</sub>H<sub>4</sub><sup>+</sup> are just formed in reactions with H<sub>2</sub><sup>+</sup>, whereas C<sub>2</sub>H<sub>5</sub><sup>+</sup> and C<sub>2</sub>H<sub>3</sub><sup>+</sup>, which are the most abundant C<sub>2</sub>H<sub>x</sub><sup>+</sup> ions, have additional and more efficient production channels.

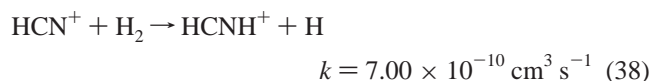
The C<sub>2</sub>H<sub>x</sub><sup>+</sup> ions do not react appreciably with molecular hydrogen, CH<sub>4</sub>, or N<sub>2</sub>, but they give rise to a series of dissociative association reactions with the lesser neutral components of the plasmas (NH<sub>3</sub> and C<sub>2</sub>H<sub>2</sub>).<sup>58,59</sup> Other minor ions are also present in this mass range. The peak at  $m/q = 28$  is due to N<sub>2</sub><sup>+</sup> in H<sub>2</sub>/N<sub>2</sub> plasmas and C<sub>2</sub>H<sub>4</sub><sup>+</sup> in H<sub>2</sub>/CH<sub>4</sub> plasmas;



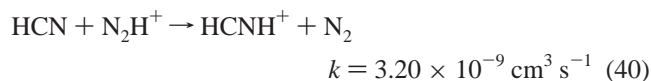
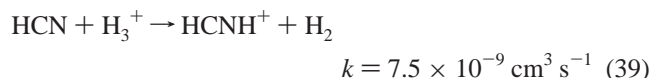
both ions are produced in very similar amounts, and the two signals add up in the  $\text{H}_2/\text{N}_2/\text{CH}_4$  discharges. A signal at mass 29 is also observed in the pure  $\text{H}_2$  plasmas. This peak corresponds most probably to  $\text{HCO}^+$  formed in the protonation with  $\text{H}_3^+$  of the CO desorbed from the chamber walls. A minor peak at mass 30, corresponding to  $^{15}\text{NNH}^+$ , is also observed in the plasmas containing  $\text{H}_2$  and  $\text{N}_2$ . An interesting question concerning the  $\text{H}_2/\text{N}_2/\text{CH}_4$  plasma mixtures is the possible appearance of mixed ions containing carbon and nitrogen. As mentioned above, addition of  $\text{N}_2$  to  $\text{H}_2/\text{CH}_4$  plasmas can inhibit formation of hydrogenated carbon films on metallic walls, which is at present a major issue in the development of next-generation controlled fusion devices.<sup>22</sup> Volatile species with C–N bonds like HCN and  $\text{C}_2\text{N}_2$  have been found in higher pressure (1.5 mbar) MW plasmas containing  $\text{H}_2$ ,  $\text{N}_2$ , and  $\text{CH}_4$  and attributed to gas-phase reactions.<sup>71,72</sup> Formation of HCN, CN, and  $\text{C}_2\text{N}_2$  has been reported too in the etching of a-C:H films in nitrogen plasmas.<sup>73</sup> Jacob and co-workers stressed the efficiency of chemical sputtering of the carbonated films by  $\text{N}_2^+$  ions<sup>24,25</sup> and showed that the erosion rate is greatly enhanced through a synergistic effect between ions, penetrating into the film and creating dangling bonds and thermal H atoms, passivating the broken bonds, and giving rise to volatile  $\text{C}_x\text{H}_x$  or  $\text{C}_x\text{N}_y\text{H}_z$  stable molecules that would diffuse to the surface and desorb.<sup>13,24–26</sup> In their  $\text{CH}_4/\text{N}_2$  plasmas those authors found indeed HCN and  $\text{C}_2\text{H}_x$  molecules in comparable concentrations.<sup>24</sup> In contrast with the  $\text{CH}_4/\text{N}_2$  plasmas just commented on, those studied here are mainly formed by  $\text{H}_2$  with only a small percentage of  $\text{CH}_4$  or  $\text{N}_2$ . Analogous chemical sputtering processes, caused in our case by  $\text{N}_2\text{H}^+$  ions, could also take place in the discharges studied in this work, but the desorbed products seem to be somewhat different. In previous studies on similar plasmas Tabarés et al.<sup>27,29</sup> found that the amount of HCN is very small as compared with that of  $\text{C}_2\text{H}_x$  hydrocarbons. This result has been recently corroborated by new and more refined experiments<sup>39</sup> using a newly developed cryo-trapping assisted mass spectrometric technique.<sup>74</sup> The present ion distribution measurements confirm this conclusion. Electron impact ionization of HCN should lead to formation of  $\text{HCN}^+$ , which would also be produced in the very efficient charge-transfer reaction



This ion could, in principle, contribute to the signal at  $m/q = 27$ , but it is readily transformed to  $\text{HCNH}^+$  in collisions with  $\text{H}_2$



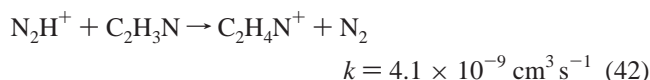
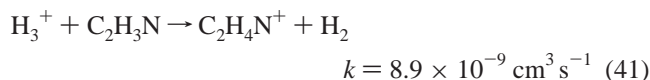
Protonation of HCN with  $\text{H}_3^+$  and  $\text{N}_2\text{H}^+$  would also lead to production of  $\text{HCNH}^+$



The major species ( $\text{H}_2$ ,  $\text{N}_2$ , and  $\text{CH}_4$ ) in the discharge do not react with  $\text{HCNH}^+$ ,<sup>51</sup> and thus, this ion should give a significant contribution to the peak at  $m/q = 28$  in mixed  $\text{H}_2/\text{N}_2/\text{CH}_4$  plasmas. Inspection of Figure 4, keeping in mind reactions 37–40, rules out a noticeable presence of HCN in the plasmas

studied: The peak at mass 27, attributed to  $\text{C}_2\text{H}_3^+$  in  $\text{H}_2/\text{CH}_4$  plasmas, does not change with addition of  $\text{N}_2$ , and the peak at mass 28 in mixed  $\text{H}_2/\text{N}_2/\text{CH}_4$  plasmas corresponds roughly to the sum of the  $\text{N}_2^+$  and  $\text{C}_2\text{H}_4^+$  signals in the  $\text{H}_2/\text{N}_2$  and  $\text{H}_2/\text{CH}_4$  discharges respectively. No hints about formation of CN or  $\text{C}_2\text{N}_2$ , also typical products of the nitrogen etching, are found in the ion chemistry. The CN radical has been identified via emission spectroscopy, but its concentration must be very small. As for cyanogen, no traces of the primary ion or of its protonated  $\text{C}_2\text{N}_2\text{H}^+$  derivative were found in the measurements. It seems that in the plasmas dominated by  $\text{H}_2$  with only small amounts of nitrogen chemical sputtering or other possible mechanisms of carbon film removal would lead almost exclusively to  $\text{C}_x\text{H}_y$  desorbed species.<sup>39</sup> Nevertheless, some evidence for C–N bond formation is discussed below.

**Ions of Masses 39–45.** Beyond  $m/q = 30$  all ions found contain carbon, and most of them are produced in dissociative association processes analogous to those shown in the previous paragraphs. A group of weak signals due to  $\text{C}_3\text{H}_x^+$  is found between 39 and 43. The peak at  $m/q = 45$ , found even in the pure  $\text{H}_2$  plasmas, is due to  $\text{HCO}_2^+$  generated in protonation reactions of the traces of  $\text{CO}_2$  present as an impurity in the vessel. Although ions in this mass range are produced in very small amounts, their concentration is enriched in the plasma due to the slower flow of heavier ions to the cathode commented on above. The most intense peak in this mass range appears at  $m/q = 42$  in plasmas of the  $\text{H}_2/\text{N}_2/\text{CH}_4$  ternary mixture and is mostly due to protonated acetonitrile,  $\text{C}_2\text{H}_4\text{N}^+$ . This is the only C/N mixed ion identified in the plasmas under study. As can be seen, this peak, attributed to  $\text{C}_3\text{H}_6^+$  in  $\text{H}_2/\text{CH}_4$  plasmas, increases by an order of magnitude upon incorporation of  $\text{N}_2$ . The  $\text{C}_2\text{H}_4\text{N}^+$  ion is formed probably through protonation of acetonitrile.



Protonated acetonitrile does not react with hydrogen<sup>58,59</sup> and due to its comparatively high mass tends to concentrate in the plasma. In the  $\text{H}_2\text{CH}_4/\text{N}_2$  plasma of this work  $\text{C}_2\text{H}_4\text{N}^+$  ions make about 1% of the total ion density. Its stability against  $\text{H}_2$  makes it a good candidate for observation in the interstellar medium and has in fact been sought, but it has not been unambiguously identified thus far.<sup>6,75</sup> Production of  $\text{C}_2\text{NH}_x$  species in radical–molecule reactions has been reported previously in RF and MW  $\text{N}_2/\text{CH}_4$  discharges.<sup>51,52</sup> Under the conditions of the present experiments, with low gas-phase collision frequency, formation of  $\text{C}_2\text{H}_3\text{N}$  is most probably due to surface reactions between carbon- and nitrogen-containing radicals and molecules. In a recent work<sup>39</sup> analogous processes involving heterogeneous reactions of carbon radicals with nitrogen-containing molecules at the film surface, leading also to production of  $\text{C}_2\text{NH}_x$  species, have been advanced as a likely way for the effective scavenging of radical growth precursors for formation of a-C:H layers in  $\text{H}_2/\text{N}_2/\text{CH}_4$  plasmas, a mechanism of C-film growth inhibition complementary to that of chemical sputtering mentioned earlier.

## 5. Summary and Conclusions

The laboratory investigation of cold plasmas in which  $\text{H}_2$  is predominant can be of great interest for identification of species

and processes of likely relevance in interstellar space, ionospheres of the giant planets, or controlled fusion devices.

In this work we studied the ion composition of the plasmas formed in low-pressure (0.02 mbar) hollow cathode discharges of H<sub>2</sub> with small admixtures (5%) of CH<sub>4</sub> and N<sub>2</sub>. The mass distributions of ions in these plasmas are not dominated by the primary products of electron impact ionization but are rather determined by a rich ion–molecule chemistry dominated by protonation reactions. In all cases the H<sub>3</sub><sup>+</sup> ion is found to be prevalent, but its concentration is significantly depleted in plasmas containing CH<sub>4</sub> and, most notably, in those containing N<sub>2</sub>, where it gives rise to the N<sub>2</sub>H<sup>+</sup> ion. In spite of the small proportion of N<sub>2</sub> in the plasma, this ion can reach concentrations comparable to those of H<sub>3</sub><sup>+</sup> due partly to its comparatively small flow velocity toward the cathode derived from its larger mass. Both H<sub>3</sub><sup>+</sup> and N<sub>2</sub>H<sup>+</sup> are very good protonating agents that react efficiently with hydrocarbons. Among the host of ions, other than H<sub>x</sub><sup>+</sup>, found in the plasmas studied, N<sub>2</sub>H<sup>+</sup>, CH<sub>5</sub><sup>+</sup>, NH<sub>4</sub><sup>+</sup>, and CH<sub>3</sub><sup>+</sup> (in that order) have the highest concentrations followed by C<sub>2</sub>H<sub>5</sub><sup>+</sup> and C<sub>2</sub>NH<sub>4</sub><sup>+</sup>. Note the prevalence of hydrocarbon ions with odd hydrogen numbers resulting from protonation. All of these major ions are relatively unreactive with H<sub>2</sub> and should thus be relatively stable in the interstellar medium. Two of them, H<sub>3</sub><sup>+</sup> and N<sub>2</sub>H<sup>+</sup>, have in fact been observed, and the present results corroborate that the rest, which are assumed in many astrochemistry models, constitute good candidates for astronomical surveys.

Given the configuration of the discharges studied, with the cathode acting as an effective positive charge sink, all ions observed are formed in the glow region and can give valuable clues about their neutral precursors. The only C/N mixed ion identified in the H<sub>2</sub>/CH<sub>4</sub>/N<sub>2</sub> mixtures is C<sub>2</sub>NH<sub>4</sub><sup>+</sup>, which indicates that acetonitrile, its precursor, is formed in wall reactions between nitrogen- and carbon-containing species. On the other hand, no ions derived from HCN are found in the analysis of the ion distributions, which suggests that hydrogen cyanide is not formed in appreciable amounts.

Although the comparison of the ion distributions of the various discharges investigated in this study provides an approximate global picture of their ion chemistry, further work will be needed for a full understanding of the detailed mechanisms.

**Acknowledgment.** We are indebted to F. Hempel, A. von Keudell, and J. P. van Helden for providing us with refs 72, 42, and 56, respectively. J. M. Castillo, M. A. Moreno, and J. Rodriguez provided valuable technical assistance for which we are grateful. This work was supported by the Ministry of Education of Spain under grants ENE2006-14577, FIS2004-00456, and FTN2003-08228.

## References and Notes

- (1) McCall, B. J.; Oka, T. *Science* **2000**, 287, 1941.
- (2) Oka, T. *The Ubiquitous H<sub>3</sub><sup>+</sup>*; Springer Proceedings in Physics; Springer: New York, 2004; p 37.
- (3) Milligan, D. B.; Wilson, P. F.; Freeman, C. G.; Meot-Ner (Mautner), M.; McEwan, M. J. *J. Phys. Chem. A* **2002**, 106, 9745.
- (4) Herbst, E. *Chem. Soc. Rev.* **2001**, 30, 168.
- (5) Herbst, E. *J. Phys. Chem. A* **2005**, 109, 4017.
- (6) Petrie, S.; Bohme, D. K. *Mass Spectrom. Rev.* **2007**, 26, 258.
- (7) Majed, T.; Waite, J. H.; Bougher, S. W.; Yelle, R. V.; Gladstone, G. R.; McConell, J. C.; Bhardwaj, A., Jr. *Adv. Space Res.* **2004**, 33, 197.
- (8) Jacob, W. *Thin Solid Films* **1998**, 326, 1.
- (9) Grill, A. *Diamond Relat. Mater.* **1999**, 8, 428.
- (10) Lombardi, G.; Hassouni, K.; Stancu, G.-D.; Mechold, L.; Röpcke, J.; Giquel, A. *J. Appl. Phys.* **2005**, 98, 053303.
- (11) Gordillo-Vázquez, F. J.; Herrero, V. J.; Tanarro, I. *Chem. Vap. Deposition* **2007**, 13, 267.
- (12) Teii, K.; Hori, M.; Goto, T. *J. Appl. Phys.* **2002**, 92, 4103.
- (13) Hopf, C.; von Keudell, A.; Jacob, W. *J. Appl. Phys.* **2003**, 93, 3352.
- (14) Jacob, W.; Hopf, C.; von Keudell, A.; Meier, M.; Schwarz-Selinger, T. *Rev. Sci. Instrum.* **2003**, 74, 5123.
- (15) Morrison, N. A.; William, C.; Milne, W. I. *J. Appl. Phys.* **2003**, 94, 7031.
- (16) Bauer, M.; Schwarz-Selinger, T.; Jacob, W.; von Keudell, A. *J. Appl. Phys.* **2005**, 98, 073302.
- (17) De Bleecker, K.; Bogaerts, A.; Goedheer, W. *Phys. Rev. E* **2006**, 73, 026405.
- (18) Liu, A. Y.; Cohen, M. L. *Science* **1989**, 245, 841.
- (19) Weber, F. R.; Oechsner, H. *Thin Solid Films* **1999**, 355, 73.
- (20) Tabarés, F. L.; Rohde, V.; the ASDEX upgrade team. *Plasma Phys. Control. Fusion* **2004**, 46, B381.
- (21) Federici, G.; Skinner, C. H.; Brooks, J. N.; Coad, J. P.; Grisolia, G.; Haasz, A. A.; Hassanein, A.; Philipps, V.; Pitcher, C. S.; Roth, J.; Wampler, W. R.; Whyte, D. G. *Nucl. Fusion* **2001**, 41, 1967.
- (22) Counsell, G.; Coad, P.; Grisolia, C.; Hopf, C.; Jacob, W.; Kirshner, A.; Kreter, A.; Krieger, K.; Likonen, J.; Philipps, V.; Roth, J.; Rubel, M.; Salancon, E.; Semerok, E.; Tabares, F. L.; Widdowson, A.; JET EFDA contributors. *Plasma Phys. Control. Fusion* **2006**, 48, B189.
- (23) Tabarés, F. L.; Tafalla, D.; Rohde, V.; Stamp, M.; Mathews, G.; Esser, G.; Philipps, V.; Doerner, R.; Baldwin, M. *J. Nucl. Mater.* **2005**, 337–339, 867.
- (24) Jacob, W.; Hopf, C.; Schlüter, M.; Schwarz-Selinger, T.; Sun, C. *Optimisation of hydrocarbon redeposition reduction by tokamak-compatible scavenger techniques*; EFDA Task TW3-TPP-SCAVOP, subtask 2; Final report, 2004.
- (25) Jacob, W.; Hopf, C.; Schlüter, M. *Appl. Phys. Lett.* **2005**, 86, 201103.
- (26) Jacob, W.; Hopf, C.; Schlüter, M. *Phys. Scr.* **2006**, T124, 32.
- (27) Tabarés, F. L.; Tafalla, D.; Tanarro, I.; Herrero, V. J.; Islyaikin, A.; Maffiotte, C. *Plasma Phys. Control. Fusion* **2002**, 44, L37.
- (28) Tabarés, F. L.; Tafalla, D. *Phys. Scr.* **2003**, T103, 47.
- (29) Tabarés, F. L.; Tafalla, D.; Tanarro, I.; Herrero, V. J.; Islyaikin, A. M. *Vacuum* **2004**, 73, 161.
- (30) Schwarz-Selinger, T.; Hopf, C.; Sun, C.; Jacob, W. *J. Nucl. Mater.* **2007**, 363, 174.
- (31) Shakhmatov, V. A.; De Pascale, O.; Capitelli, M.; Hassouni, K.; Lombardi, G.; Gicquel, A. *Phys. Plasmas* **2005**, 12, Art No 073301.
- (32) Lavrov, B. P.; Melnikov, A. S.; Käning, M.; Röpcke, J. *Phys. Rev. E* **1999**, 59, 3526.
- (33) Qing, Z.; Otorbaev, D. K.; Brussaard, G. J. H.; van de Sanden, M. C. M. *J. Appl. Phys.* **1996**, 80, 1312.
- (34) Lavrov, B. P.; Osiac, M.; Pipa, A. V.; Röpcke, J. *Plasma Sources Sci. Tech.* **2003**, 12, 576.
- (35) Pigarov, A. Yu. *Phys. Scr.* **2002**, T96, 16.
- (36) Loureiro, J.; Ferreira, C. M. *J. Phys. D: Appl. Phys.* **1989**, 22, 1680.
- (37) Hollman, E. M.; Pigarov, A. Yu. *Phys. Plasmas* **2002**, 9, 4330.
- (38) Méndez, I.; Gordillo-Vázquez, F. J.; Herrero, V. J.; Tanarro, I. *J. Phys. Chem. A* **2006**, 110, 6060.
- (39) Tabarés, F. L.; Ferreira, J. A.; Tafalla, D. *Chem. Vap. Deposition* **2007**, 13, 335.
- (40) Castillo, M. Ph.D. Thesis, Espectrometría y cinética de plasmas fríos de óxidos de nitrógeno y aire, Madrid, Spain, 2004.
- (41) Castillo, M.; Méndez, I.; Islyaikin, A. M.; Herrero, V. J.; Tanarro, I. *J. Phys. Chem. A* **2005**, 109, 6225.
- (42) Pecher, P. Ph.D. Thesis, Quantitative Determination of the Particle Fluxes Emanating from Methane ECR Plasmas, Max-Planck-Institut Für Plasmaphysik, 1998.
- (43) Okada, K.; Komatsu, S. *J. Appl. Phys.* **1998**, 84, 6923.
- (44) de los Arcos, T.; Domingo, C.; Herrero, V. J.; Sanz, M. M.; Schulz, A.; Tanarro, I. *J. Phys. Chem. A* **1998**, 102, 6282.
- (45) Castillo, M.; Herrero, V. J.; Tanarro, I. *Plasma Sources Sci. Tech.* **2002**, 11, 368.
- (46) Lieberman, M. A.; Lichtenberg, A. J. *Principles of plasma discharges and materials processing*; John Wiley & Sons: New York, 1994.
- (47) Wronski, Z. *Vacuum* **1989**, 39, 941.
- (48) Kang, D. H.; Preuss, R.; Schwarz-Selinger, T.; Dose, V. *J. Mass Spectrom.* **2002**, 37, 748.
- (49) Misina, M.; Pokorný, P. *Surf. Coat. Technol.* **2003**, 173, 914.
- (50) Dolezal, V.; Dvorak, P.; Janca, J. *Czech. J. Phys.* **2006**, 56, B697.
- (51) Mutsukura, N. *Plasma Chem. Plasma Process.* **2001**, 21, 265.
- (52) Kareev, M.; Sablier, M.; Fujii, T. *J. Phys. Chem. A* **2000**, 104, 7218.
- (53) Gordiets, B.; Ferreira, C. M.; Pinheiro, M. J.; Ricard, A. *Plasma Sources Sci. Technol.* **1998**, 7, 363.
- (54) Gordiets, B.; Ferreira, C. M.; Pinheiro, M. J.; Ricard, A. *Plasma Sources Sci. Technol.* **1998**, 7, 379.
- (55) Tatarova, E.; Dias, F. M.; Gordiets, B.; Ferreira, C. M. *Plasma Sources Sci. Technol.* **2005**, 14, 19.

- (56) van Helden, J. P., Ph.D. Thesis, The generation of molecules through plasma-surface interactions, Eindhoven University, The Netherlands, 2006.
- (57) Matyash, K.; Schneider, R.; Bergmann, A.; Jacob, W.; Fantz, U.; Pecher, P. *J. Nucl. Mater.* **2003**, *313–316*, 434.
- (58) Anicich, V. G. *J. Phys. Chem. Ref. Data* **1993**, *22*, 1469.
- (59) Anicich, V. G. J.P.L. Publication 03-19, NASA, 2003.
- (60) Janev, R.; Reiter, D. Juel-Report 3966: *Collision Processes of Hydrocarbon Species in Hydrogen Plasmas: I. Methane Family* and Juel-Report 4005: *Collision Processes of Hydrocarbon Species in Hydrogen Plasmas: II. Ethane & Propane Families*, [http://www.eirene.de/html/a\\_m\\_data.html](http://www.eirene.de/html/a_m_data.html)
- (61) Tanarro, I.; de los Arcos, T.; Domingo, C.; Herrero, V. J.; Sanz, M. M. *Vacuum* **2002**, *64*, 457.
- (62) <http://physics.nist.gov/PhysRefData/Ionization/molTable.html>.
- (63) Mul, M. P.; Mitchell, J. B. A.; D'Angelo, V. S.; McGowan, J. Wm.; Froelich, H. R. *J. Phys. B: At. Mol. Phys.* **1981**, *14*, 1353.
- (64) Kossyi, I. A.; Kosstinsky, Y.; Matveyev, A. A.; Silakov, V. *Plasma Sources Sci. Technol.* **1992**, *1*, 207.
- (65) Atkinson, R.; Baulch, D. L.; Cox, R. A.; Hampson, R. F., Jr.; Kerr, J. A.; Rossi, M. J.; Troe, J. *J. Phys. Chem. Ref. Data* **1999**, *28*, 191.
- (66) Wesley, F.; Herron, J. T.; Hampson, R. F.; Mallard, W. G. Eds. *NIST Chemical Kinetics Database*; U.S. Department of Commerce: Gaithersburg, MD, 1992.
- (67) Asvany, O.; Kumar, P.; Redlich, B.; Hegemann, I.; Schlemmer, S.; Marx, D. *Science* **2005**, *309*, 1219.
- (68) Huang, X.; McCoy, A. B.; Bowman, J. B.; Johnson, L. M.; Savage, C.; Dong, F.; Nesbitt, D. J. *Science* **2006**, *311*, 60.
- (69) Ahlberg, P.; Karlsson, A.; Goepfert, A.; Nilsson Lill, S. O.; Dinér, P.; Sommer, J. *Chem. Eur. J* **2001**, *7*, 1936.
- (70) Maret, S.; Bergin, E. A.; Lada, C. J. *Nature* **2006**, *44*, 425.
- (71) Hempel, F.; Davies, P. B.; Loffhagen, D.; Mechold, L.; Röpcke, J. *Plasma Sources Sci. Technol.* **2003**, *12*, S98.
- (72) Hempel, F. Ph.D. Thesis, Absorption spectroscopy studies in low pressure non equilibrium molecular plasmas using tuneable infrared diode lasers, Greifswald, Germany, 2004.
- (73) Hong, J.; Turban, G. *Diamond Relat. Mater.* **1999**, *8*, 572.
- (74) Ferreira, J. A.; Tabarés, F. L. *J. Vac. Sci. Technol. A* **2007**, *25*, 246.
- (75) Turner, B. E.; Amano, T.; Feldman, P. A. *Astrophys. J* **1990**, *349*, 376.